ISSN 1674-1056
http://cpb.iphy.ac.cn
http://iopscience.iop.org/cpb
中国物理 B
Chinese Physics B

Absolute density measurement of nitrogen dioxide with cavity-enhanced laser-induced fluorescence

Zheng-Hai Yang(杨正海), Yong-Cheng Yang(杨永成), Lian-Zhong Deng(邓联忠), Jian-Ping Yin(印建平)

Citation: Chin. Phys. B . 2018, 27(10): 100601. **doi:** 10.1088/1674-1056/27/10/100601

Journal homepage: http://cpb.iphy.ac.cn; http://iopscience.iop.org/cpb

What follows is a list of articles you may be interested in

Laser absorption spectroscopy for high temperature H_2O time-history measurement at 2.55 μm during oxidation of hydrogen

Yu-Dan Gou(苟于单), De-Xiang Zhang(张德翔), Yi-Jun Wang(王易君), Chang-Hua Zhang(张昌华), Ping Li(李萍), Xiang-Yuan Li(李象远)

Chin. Phys. B . 2018, 27(7): 074213. **doi:** 10.1088/1674-1056/27/7/074213

ADC border effect and suppression of quantization error in the digital dynamic measurement

Li-Na Bai(白丽娜), Hai-Dong Liu(刘海东), Wei Zhou(周渭), Yong Zhang(张勇), Hong-Qi Zhai(翟鸿启), Zhen-Jian Cui(崔震健), Ming-Ying Zhao(赵明英), Xiao-Qian Gu(谷小倩), Bei-Ling Liu(刘蓓玲), Li-Bei Huang(黄李贝)

Chin. Phys. B . 2017, 26(9): 090601. **doi:** 10.1088/1674-1056/26/9/090601

Analysis of algebraic reconstruction technique for accurate imaging of gas temperature and concentration based on tunable diode laser absorption spectroscopy

Hui-Hui Xia(夏晖晖), Rui-Feng Kan(阚瑞峰), Jian-Guo Liu(刘建国), Zhen-Yu Xu(许振宇), Ya-Bai He(何亚柏)

Chin. Phys. B . 2016, 25(6): 064205. **doi:** 10.1088/1674-1056/25/6/064205

Lasing dynamics study by femtosecond time-resolved fluorescence non-collinear optical parametric amplification spectroscopy

Wei Dang(党伟), Qing Liao(廖清), Peng-Cheng Mao(毛鹏程), Hong-Bing Fu(付红兵), Yu-Xiang Weng(翁羽翔)

Chin. Phys. B . 2016, 25(5): 054207. **doi:** 10.1088/1674-1056/25/5/054207

Wavelength modulation spectroscopy at 1530.32 nm for measurements of acetylene based on Fabry-Perot tunable filter

Yun-Long Li(李运龙), Bing-Chu Yang(杨兵初), Xue-Mei Xu(许雪梅)

Chin. Phys. B . 2016, 25(2): 024208. **doi:** 10.1088/1674-1056/25/2/024208

Absolute density measurement of nitrogen dioxide with cavity-enhanced laser-induced fluorescence*

Zheng-Hai Yang(杨正海), Yong-Cheng Yang(杨永成), Lian-Zhong Deng(邓联忠)†, and Jian-Ping Yin(印建平)

State Key Laboratory of Precision Spectroscopy, School of Physics and Material, East China Normal University, Shanghai 200062, *China*

(Received 21 May 2018; revised manuscript received 10 August 2018; published online 27 September 2018)

The absolute number density of nitrogen dioxide (NO_2) seeded in argon is measured with cavity-enhanced laser-induced fluorescence (CELIF) through using a pulsed laser beam for the first time. The cavity ring down (CRD) signal is acquired simultaneously and used for normalizing the LIF signal and determining the relationship between the measured CELIF signal and the NO_2 number density. The minimum detectable NO_2 density down to $(3.6\pm0.1)\times10^8$ cm^{-3} is measured in 60 s of acquisition time by the CELIF method. The minimum absorption coefficient is measured to be $(2.0\pm0.1)\times10^{-10}$ cm^{-1}, corresponding to a noise equivalent absorption sensitivity of $(2.2\pm0.1)\times10^{-9}$ cm$^{-1}\cdot$Hz$^{-1/2}$. The experimental system demonstrated here can be further improved in its sensitivity and used for environmental monitoring of outdoor NO_2 pollution.

Keywords: cavity-enhanced laser-induced fluorescence (CELIF), cavity ring down (CRD)

PACS: 06.20.Dk, 42.62.Fi, 07.88.+y **DOI:** 10.1088/1674-1056/27/10/100601

1. Introduction

The knowledge of absolute number density of molecular samples plays an important role in many disciplines such as precision measurement,[1,2] environmental pollutants monitoring,[3] cold collision and cold chemistry.[4] Among various molecules of environmental interest, nitrogen dioxide is very attractive.[5,6] NO_x species (NO, NO_2) play a vital role in determining the photochemistry of troposphere, controlling the abundance of ozone (O_3) and OH.[7] And they have strong influences on air quality, formation of acid rain, and thus affecting all living things on the Earth.

The importance of detecting absolute number density of worthy species results in the development of a number of successful methods, which can be roughly divided into two main groups. One is the absorption method, including the differential optical absorption spectroscopy (DOAS),[8] cavity enhanced absorption spectroscopy (CEAS),[9,10] tunable diode laser absorption spectroscopy (TDLAS),[11] cavity ring down spectroscopy (CRDS)[12–15] and cavity attenuated phase shift spectroscopy (CAPS).[16] The above mentioned methods are just a few examples among the many absorption techniques. The other is the laser-induced fluorescence (LIF) method, including the single-photon LIF[17,18] and two-photon LIF.[19] Besides, sensitive measurements of NO_2 have also been achieved with the technique of photofragmentation-chemiluminescence (PF-CL).[20] In recent years, a new method called cavity-enhanced laser-induced fluorescence (CELIF) has been described by Sanders *et al.*,[21] and then used for measuring the absolute number density of SD radicals.[22] This method combines the absolute absorption capabilities of CRDS and the sensitivity of LIF. The CRDS data are used for normalizing the LIF signal to remove the influence of the laser intensity fluctuation.

The fluorescence lifetime of NO_2 depends on the pressure of the gas sample. Collisions with other molecular species in the gas sample can quench the photo-excited NO_2 from fluorescing. The ratio of the radiative rate constant to the other quenching rate constant determines the real lifetime of the NO_2 fluorescence. For instance, the radiative lifetime of NO_2 excited at $\sim$ 440 nm is $\sim$ 70 μs, and the real lifetime is estimated at $\sim$ 5 μs at a pressure of $\sim$ 0.2 Torr (1 Torr = 1.33322×10^2 Pa).[17]

The NO_2 number density fluctuates remarkably in various areas, ranging from less than 100 pptv (parts per trillion) in the rural area to more than 100 ppbv (parts per billion) in the urban atmosphere.[8,23] This density variation covers a wide range of more than six orders of magnitude. The technique of CRDS typically can cover no more than three orders of magnitude in the dynamic range in terms of absorbance measurement. The technique of CELIF can, however, extend the dynamic range of absorbance measurements compared with a sole CRDS measurement by at least three orders of magnitude.[21]

In this paper, we describe a newly-built CELIF setup with a pulsed laser source and use it as a high-sensitivity instrument for measuring the absolute number density of NO_2 samples in the laboratory. Some of the experimental details are first described. Then, the experimental results obtained with the CELIF technique are presented. Some discussion and a simple conclusion are given in the end.

*Project supported by the National Natural Science Foundation of China (Grant Nos. 11504112, 91536218, and 11604100).

†Corresponding author. E-mail: lzdeng@phy.ecnu.edu.cn

© 2018 Chinese Physical Society and IOP Publishing Ltd

2. Experiment

Figure 1 shows a conceptual drawing of our experiment setup. Survey scans of NO_2 are performed with the fundamental output of a pulsed dye laser (SirahPrecisionScan, linewidth 0.04 cm^{-1}) pumped by the third harmonic of an Nd:YAG laser (Spectra-Physics, Quanta-Ray Lab-170-10, 355 nm, repetition rate $f = 10$ Hz, pulse width 8 ns–10 ns). The dye laser is operated with Coumarin 440 dissolved in ethanol. The central portion of the laser output is first selected and then passes through a spatial filter assembly consisting of a pair of lenses (the focal length of which are $f = 150$ mm and $f = 75$ mm, respectively) positioned at 225 mm apart from a standard telescope arrangement. A 50-μm-diameter (aperture) precision pinhole is located at the focus of the telescope. The filtered laser beam is then coupled into the optical cavity through one end mirror with the help of an $f = 600$-mm lens located, and thus making the laser focus at the center of the cavity. The pulse energy of the laser shot for the following experiment is measured to be about 0.1 mJ in front of the spatial filtering assembly.

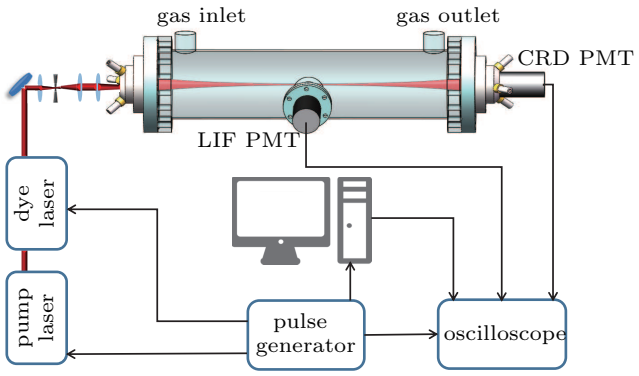


Fig. 1. (color online) Schematic diagram of the experimental setup.

The high-finesse ring-down cavity consists of two identical plano-concave reflective mirrors (Layertec) with quoted reflectivity $> 99.98\%$ at a wavelength around 440 nm. The cavity mirror is O-ring sealed to a stainless steel flange by screws. Cavity adjustment is realized by rotating three other screws of ultrafine threads from outside. The mirror substrates each have a radius of curvature of 100 cm, and they are 84 cm apart. The whole cavity assembly is located in a home-built vacuum chamber. The vacuum chamber has various ports for pressure gauges and quartz windows with a central axis collinear to the cavity axis.

Light leaking through the opposite cavity mirror is detected with a photomultiplier tube (PMT) positioned behind. A two-lens LIF detection optical system is aligned perpendicular to the cavity axis and LIF photons are collected by another PMT (H3695-10, Hamamatsu). The LIF collecting optics has a field of view that restricts the probe volume to $\sim 1.0 \times 10^{-3}$ cm^3. Only 1 cm of the total 84-cm cavity length is detected. The wavelength of the NO_2 fluorescence extends from visible to infrared. To avoid interfering from the pump laser of 440 nm, such as chamber and Rayleigh scattering, a long-pass optical filter of $\lambda > 495$ nm is placed in front of the LIF PMT. The CRDS and LIF signals are simultaneously acquired via a digital oscilloscope and sent to a host PC for later processing.

Following the cavity alignment, a mechanical pump and a turbomolecular pump keep the pressure in the vacuum chamber typically below 4×10^{-6} Torr, which is measured by an ion gauge. Bellows are adopted to minimize the influence of mechanical vibration from both pumps on the system stability. Then the turbomolecular pump is closed and the gas sample is introduced into the chamber via a flange connected dosing valve. The gas sample enters into the chamber continuously and is pumped away by the mechanical pump. A gas flow of constant low pressure is maintained in the chamber by concerted work of the dosing valve and an angle valve in front of the mechanical pump. The temperature of the flowing gas sample is ~ 293 K.

The total volume of our sample cavity is estimated at about 2500 cm^3. The flow rate of the dry gas mixture controlled by the dosing valve (INFICON VDH040-U) is about 20 sccm. The gas flows through the sample cavity under essentially plug flow conditions that are distorted by the gas entering into and leaving from the cell at right angle to the cavity axis. The residence time of the gas sample is about 2 s inside the cavity with a pressure of ~ 0.2 Torr. Compared with static samples, flowing gas samples have some prominent advantages. Firstly, the walls of the chamber will adsorb some NO_2 during the experiment, so the optical absorption of a static sample declines on a timescale of a few minutes, which is confirmed in our experiment. Secondly, a flowing gas sample provides sufficient fresh molecules to be excited by the 440-nm laser.

The gas mixture of NO_2 /Ar (each with a purity of $\sim 99.9\%$) is first prepared in a 1-L gas mixing bottle with a total pressure of ~ 4560 Torr (i.e., 0.6 MPa with NO_2/Ar= 0.01/0.59 in pressure). Starting from this concentration, the mole fraction of NO_2 is lowered by sequential dilution. For each dilution, a fraction ($\sim 2/3$) of the gas mixture is pumped away and Ar is added to restore the total pressure back to the initial value. After each dilution, the gas mixture is fully mixed for about 20 min by using convection currents generated through heating two loops of pipe of unequal length connected to the gas mixing bottle. Both the chamber and the gas feeding pipeline to the dosing valve are fully evacuated prior to each dilution.

3. Experiment results

For quantitative gas-phase absorption measurement in cavity ring-down setup, the CRDS time constants of the cavity without and with the absorbing species can be expressed as $\tau_0 = l/[c(1-R)]$ and $\tau = l/[c(1-R+\alpha l)]$, respectively. Here l is the length of the cavity, R is the reflectivity of the cavity mirror, c is the speed of light, α is the absorption coefficient of the sample in the cavity and given as $\alpha = \rho \cdot \sigma$ with σ being the absorption cross section of the sample and ρ being the sample concentration. If the cavity is filled with absorbing molecules, then the relationship between the number density of the molecules and their absorption cross section can be given as

$$\rho = \frac{1}{c}\frac{1}{\sigma}\left(\frac{1}{\tau} - \frac{1}{\tau_0}\right). \quad (1)$$

The absorption spectrum of the NO_2 is first studied with CRDS. The laser is scanned from 436.5 nm to 447.0 nm in steps of 0.04 nm in wavelength. Laser spectroscopy studies have ascribed the NO_2 absorption in a range of 430 nm–450 nm to the two electronic transitions, i.e., $^2B_2 \leftarrow {}^2A_1$ and $^2B_1 \leftarrow {}^2A_1$.[24] The initial gas mixture is diluted twice following the procedure described above before being introduced into the vacuum chamber via the dosing valve. The pressure is kept at ~ 0.2 Torr (1 Torr $= 1.33322 \times 10^2$ Pa) in the cavity chamber, which is monitored by a thermocouple gauge. For CRDS, the temporal decay of the light intensity inside the high-finesse cavity for each laser pulse is fitted with an exponential to obtain the CRDS amplitude A^{CRD} and time constant τ. Each data point is the averaged value over 20 laser shots. Then, the cavity chamber is evacuated to below 4×10^{-6} Torr using the turbo-molecular pump. After that, the chamber is filled with flowing pure dry Ar gas of ~ 0.2 Torr. The laser is scanned again over the same laser wavelength to obtain the CRDS time constant τ of the background, which incorporates the effects of mirror reflectivity, scattering from the gas sample and chamber walls, etc. The LIF signal of excited NO_2 molecules is simultaneously detected and processed by using the photon-counting mode. It is used under the conditions in which the photon-induced signals are so weak and scattered that the integration area method fails to produce reliable result. It also requires that the scattered signals be sparse enough so that they can be well ascertained. That is why we dilute the initial gas mixture twice prior to starting the measurement. Figure 2 shows the simultaneously recorded CRD (upper panel) and LIF transients (lower panel) at ~ 440 nm. The CRD time constants are ~ 5.239 μs and ~ 9.221 μs for the cases of NO_2/Ar mixture and pure Ar, respectively. The number of photon counts for the Ar background is ~ 0.15 per laser shot.

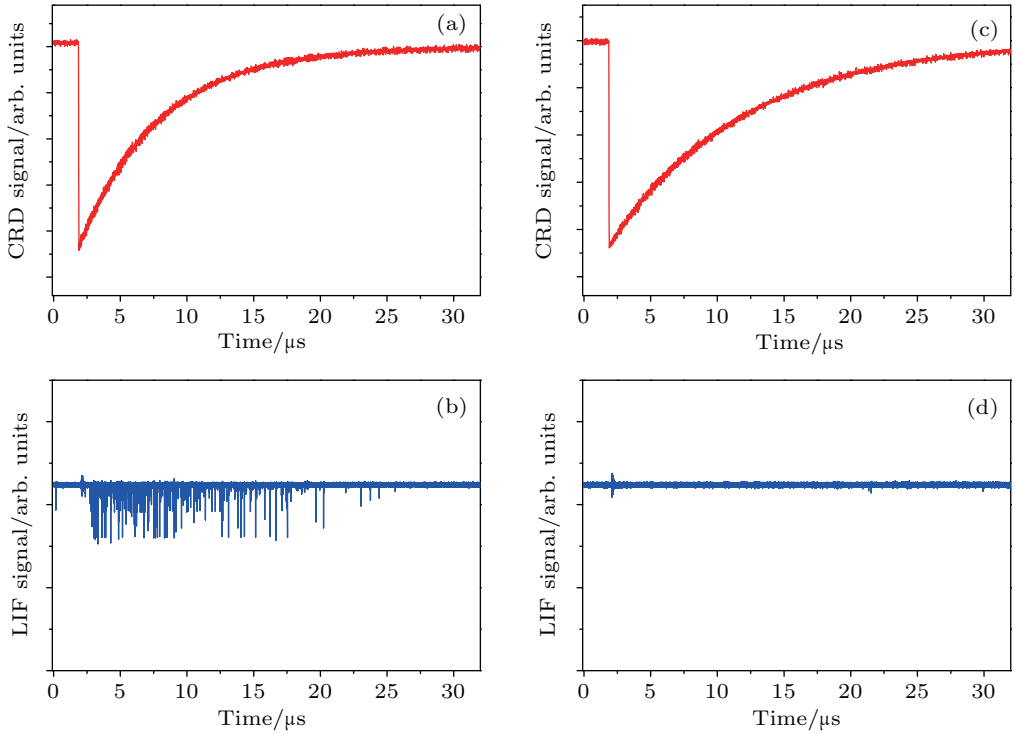


Fig. 2. (color online) Simultaneously recorded CRD [(a) and (c)] and LIF transients [(b) and (d)] at ~ 440 nm. Panels (a) and (b) correspond to the NO_2/Ar mixture; panels (c) and (d) correspond to pure Ar background. CRD time constants are (a) ~ 5.239 μs and (b) ~ 9.221 μs.

Figure 3(a) shows the corresponding absorption spectrum of NO_2 from CRDS, which agrees well with those studied before[25,26] in profile but with better resolution. The absorption cross section (σ) of NO_2 has been intensively studied in previous work. The number density of NO_2 in the cavity chamber for this measurement is calculated to be $\sim 4.9 \times 10^{12}$ cm^{-3} from Eq. (1), with an absorption cross section of $\sigma = \sim 5.66 \times 10^{-19}$ cm^2 [27] used. To remove the influence

of laser shot-to-shot fluctuation on the LIF signal, the product of A^{CRD} and τ, $I^{\mathrm{CRD}} = A^{\mathrm{CRD}} \cdot \tau$, is used to normalize the LIF signal. Here A^{CRD} and τ are, respectively, the amplitude and the time constant of the exponential fit to the CRDS trace in the presence of the gas sample. This time-integrated value of I^{CRD} contains the information about the laser intensity exciting the gas sample. The normalized LIF signal S^{CELIF} is given as $S^{\mathrm{CELIF}} = S^{\mathrm{LIF}}/I^{\mathrm{CRD}}$, and is called CELIF signal later. The normalization ensures that neither any shot-to-shot instability nor long-term drift in the probe laser pulse energy can contribute to the noise in S^{CELIF}. The LIF signal in the presence of pure Ar is processed similarly and taken as the CELIF background. Thus, the CELIF signal originating from NO_2 molecules, $S^{\mathrm{CELIF}}_{\mathrm{NO_2}}$, is obtained to be

$$S^{\mathrm{CELIF}}_{\mathrm{NO_2}} = S^{\mathrm{CELIF}}_{\mathrm{T}} - S^{\mathrm{CELIF}}_{\mathrm{BG}}. \tag{2}$$

Here, $S^{\mathrm{CELIF}}_{\mathrm{T}}$ is the total CELIF signal of the NO_2/Ar mixture and $S^{\mathrm{CELIF}}_{\mathrm{BG}}$ is the background signal for pure Ar. Figure 3(b) shows the corresponding CELIF spectrum of NO_2. As one can see, the LIF spectrum agrees well with that of the CRDS.

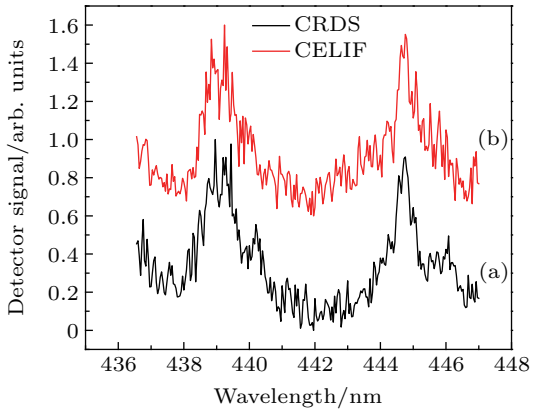


Fig. 3. (color online) (color online) (a) Absorption and (b) LIF spectrum of NO_2. Flowing gas sample keeps pressure in the cavity chamber at 0.2 Torr.

Since the LIF signal is normalized by the time-integrated CRD laser intensity to remove the influence of its fluctuation, the LIF measurement has to take place in a regime where the fluorescence of NO_2 is linearly proportional to the probe laser pulse energy. Figure 4 shows the linear dependence of the NO_2 LIF signal on the probe laser pulse energy as measured by the time-integrated ring down signal. The measurements are performed with the gas mixture diluted 7 times after first preparation. The solid squares are the experimentally measured results with the solid line being a linear fit. The arrow indicates the laser pulse energy selected for our CELIF measurements, which falls in the linear regime of the relationship.

As is well known, the CRDS method has the ability to determine the absolute density of trace gas by measuring its absorbance of the incident light, once the corresponding absorption cross section is known as can be seen from Eq. (1). Its limit to detection (LOD) is determined by minimizing the absorbance that can be reliably measured. As an absorption method, its LOD inevitably suffers the strong background laser signal that is always present. The LIF method, however, can work with a nearly background free situation, and thus offering even higher detection sensitivity and much lower LOD. The LIF signal depends on a number of experimental factors, like the number density of the absorbing sample, the laser intensity for excitation, the fluorescence quantum yield of the molecule, the efficiency of fluorescence detection, etc. Extracting the number density information of the absorbing sample from the sole LIF signal needs the knowledge of all other factors, some of which is usually difficult to obtain for a practical experiment. However, this problem with LIF measurement can be circumvented with the help of the CRDS information. Our idea to solve this problem is explained as follows.

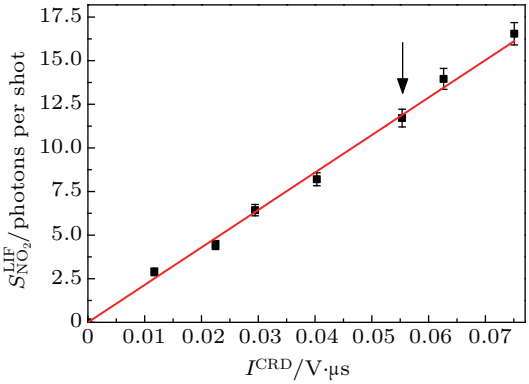


Fig. 4. (color online) Dependence of averaged LIF signal per shot on probe laser pulse energy as measured by time-integrated ring down signal. Error bar indicates shot-to-shot fluctuation of laser pulse energy, which is measured to be ~ 7%. Arrow indicates laser energy selected for our CELIF experiment.

For the CRDS measurement, equation (1) can be rearranged as

$$\Delta\tau/\tau = \rho(\sigma \cdot c \cdot \tau_0) = \rho \cdot k_1, \tag{3}$$

with $\Delta\tau = \tau_0 - \tau$ and $k_1 = \sigma \cdot c \cdot \tau_0$. The LIF signal after appropriate background subtraction is determined by the following expression:

$$S^{\mathrm{LIF}} \propto \rho \cdot V \cdot n_1 \cdot n_2 \cdot n_3 \cdot \ldots = \rho \cdot k_2, \tag{4}$$

where ρ is the number density of the molecules, V the probe volume, n_1 the ratio of molecules excited by laser, n_2 the quantum yield of the fluorescence from excited molecules, n_3 the fluorescence detection efficiency (including the solid angle for fluorescence collection, the quantum efficiency of the PMT, etc.). For our case considered here, the collisions from Ar are a dominating factor in quenching and limiting fluorescence quantum yield of NO_2. And collisions between NO_2 molecules play only an ignorable role since their concentration is so tiny compared to that of Ar. The fluorescence quantum yield of NO_2 is thus taken as a constant. The product of all the

factors is represented by k_2 for simplicity of discussion. For CELIF signal, equation (4) can be modified as

$$S_{NO_2}^{CELIF} = \frac{S^{LIF}}{I^{CRD}} = \frac{1}{I^{CRD}} \cdot \rho \cdot k_2 = \rho \cdot k_3. \quad (5)$$

Here I^{CRD} is the time-integrated CRD laser intensity which was introduced above. During the first several dilutions the concentration of NO_2 in the cavity chamber is still large enough for both the CRDS and LIF measurements to produce reliable results. One has a relationship of

$$k_3 = \frac{S_{NO_2}^{CELIF}}{\Delta\tau/\tau} k_1$$

from Eqs. (3) and (5).

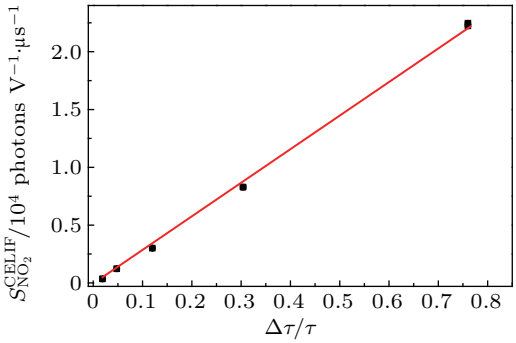


Fig. 5. (color online) Relationship between $\Delta\tau/\tau$ and $S_{NO_2}^{CELIF}$. Concentration of NO_2 molecules gradually decreased by consecutively diluting the gas sample 5 times. The statistical error bars for both the horizontal (x-axis) and vertical (y-axis) quantities are smaller than symbol size.

Figure 5 shows the relationship between the values of $S_{NO_2}^{CELIF}$ and $\Delta\tau/\tau$ measured experimentally. The gas mixture is first diluted twice after preparation and before being put into use. The concentration of NO_2 molecules gradually decreases by consecutively diluting the gas sample 5 times more. For each dilution the measurement is averaged over 600 laser shots. The probe laser is fixed at 440 nm. As one can see, good linearity is obtained for the relationship between $S_{NO_2}^{CELIF}$ and $\Delta\tau/\tau$ with the ratio $S_{NO_2}^{CELIF}/(\Delta\tau/\tau)$ (i.e. the slope) being $\sim 2.91\times10^4$. According to Eqs. (3) and (5), the relationship between the molecule density and the value of the signal $S_{NO_2}^{CELIF}$ can be expressed as

$$\rho = \sim 2.19\times10^8 \times S_{NO_2}^{CELIF}\ cm^{-3}. \quad (6)$$

With the increase of dilution times, the NO_2 concentration gradually decreases below the LOD of our CRDS measurement, which is estimated at about 7.7×10^9 cm^{-3} from the standard deviation (~ 0.011 μs) of CRDS time constant τ (~ 9.221 μs). The CRDS fails to provide reliable results, but the LIF measurement continues to work well for a few more dilutions before reaching its LOD. Figure 6 shows the relationship between the measured value of $S_{NO_2}^{CELIF}$ and the dilution times and the scattered symbols with error bar correspond to experimental results. The right axis indicates the corresponding number density of NO_2 measured.

The noise in $S_{NO_2}^{CELIF}$ is processed in the following way:[22]

$$\delta S_{NO_2}^{CELIF} = \left[\left(\delta S_T^{CELIF}\right)^2 + 2\left(\delta S_{BG}^{CELIF}\right)^2\right]^{1/2}, \quad (7)$$

$$\delta S_{BG}^{CELIF} = \left[1/(nS_{BG}^{LIF}) + \beta(I)^2\right]^{1/2} S_{BG}^{CELIF}. \quad (8)$$

The first factor in the bracket on the right-hand side of Eq. (8) corresponds to the quantum noise from LIF photon counting. $\beta(x) = \delta x/x$, represents the relative error of the fitted value x and $\beta(I) = \sqrt{\beta(A)^2 + \beta(\tau)^2}$. The LOD of the CELIF signal can be approximately calculated from Eqs. (7) and (8) and given as $S_{NO_2}^{CELIF,LOD} = \delta S_{NO_2}^{CELIF} \approx \sqrt{3}\delta S_{BG}^{CELIF}$. The horizontal dash line A in Fig. 6 indicates the LOD of our measurement in 60 s of acquisition time with $S_{NO_2}^{CELIF,LOD} = \sim 0.52$ photons $V^{-1}\cdot\mu s^{-1}$ and signal-to-noise ratio of unity. According to Eq. (6), this detection limit indicates an NO_2 density of $\sim 1.2\times10^8$ cm^{-3}. In analytical chemistry, the signal-to-noise ratio of 3 is usually required. The corresponding minimum detectable density of NO_2 is now $(3.6\pm0.1)\times10^8$ cm^{-3}. The minimum detectable absorption coefficient α^{LOD} is measured to be $(2.0\pm0.1)\times10^{-10}$ cm^{-1}, with $\sigma = (5.66\pm0.2)\times10^{-19}$ cm^2 being used, corresponding to a noise equivalent absorption (NEA) sensitivity for the system, expressed as

$$\begin{aligned} NEA &= \alpha^{LOD} \times (2n/f_{rep})^{1/2} \\ &= (2.2\pm0.1)\times10^{-9}\ cm^{-1}\cdot Hz^{-1/2}. \end{aligned} \quad (9)$$

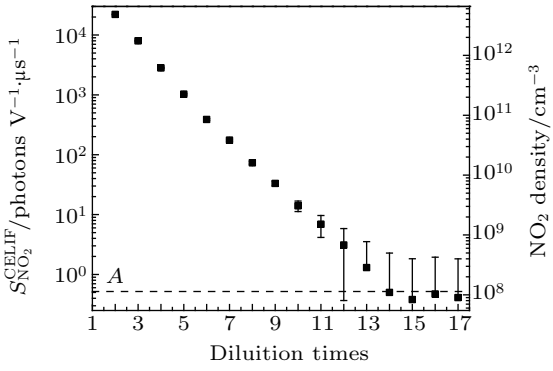


Fig. 6. Determination of LOD of our CELIF measurement of NO_2.

4. Conclusions

In this work, we measure in laboratory the absolute number density of NO_2 seeded in Ar with cavity-enhanced laser-induced fluorescence (CELIF) through using a pulsed laser beam at 440 nm. The cavity ring down (CRD) signal is acquired simultaneously and used for normalizing the LIF signal and calibrating the relationship between the measured CELIF signal and the NO_2 number density. With the decrease of the NO_2 concentration, the CRDS reaches its limit of detection

and fails to provide reliable information but the CELIF proceeds to work well for a few more dilutions before approaching to its detection limit. In 60 s of acquisition time, the minimum NO_2 number density is measured by the CELIF method to be $(3.6 \pm 0.1) \times 10^8$ cm^{-3}, corresponding to a minimum detectable absorption coefficient of $(2.0 \pm 0.1) \times 10^{-10}$ cm^{-1} and a noise equivalent absorption (NEA) sensitivity of $(2.2 \pm 0.1) \times 10^{-9}$ cm^{-1}·Hz$^{-1/2}$ for the system. For our case here, the sample absorption length for CRDS is ~ 84 cm and that for CELIF collection is only ~ 1 cm. For equal sample absorption length, like in the cases of molecular beams, the sensitivity of the CELIF will be about 3–4 orders of magnitude better than that of the CRDS measurement. In fact, there is still much room for improving our experimental setup. For example, an even larger solid angle for better fluorescence collection and a blackened chamber wall for less scattered light of background will further reduce the limit of detection. In principle, the CRDS calibration method introduced here can be applied to the CELIF measurement of other trace gas mixtures of similar conditions. But for outdoor measurements in more complicated conditions, other methods are needed to reliably explain the trace gas concentration from the LIF signal. Compared with a CELIF experiment using a continuous wave laser, the pulsed CELIF experiment is easier in cavity alignment and more convenient to operate. The scheme experimentally demonstrated in our laboratory here can be further improved and used for environmentally monitoring the outdoor NO_2 pollution.

References

[1] Hudson J J, Kara D M, Smallman I J, Sauer B E, Tarbutt M R and Hinds E A 2011 *Nature* **473** 493

[2] Cheng C F, Sun Y R and Hu S M 2015 *Chin. Phys. B* **24** 053301

[3] Stone D, Whalley L K and Heard D E 2012 *Chem. Soc. Rev.* **41** 6348

[4] Hudson E R, Ticknor C, Sawyer B C, Taatjes C A, Lewandowski H J, Bochinski J R, Bohn J L and Ye J 2006 *Phys. Rev. A* **73** 063404

[5] Delon A, Georges R and Jost R 1995 *J. Chem. Phys.* **103** 7740

[6] Richter A, Burrows J P, Nüß H, Granier C and Niemeier U 2005 *Nature* **437** 129

[7] Logan J A, Prather M J, Wofsy S C and McElroy M B 1981 *J. Geophys. Res.* **86** 7210

[8] Thornton J A, Wooldridge P J, Cohen R C, Williams E J, Hereid D, Fehsenfeld F C, Stutz J and Alicke B 2003 *J. Geophys. Res.* **108** 4496

[9] Washenfelder R A, Attwood A R, Flores J M, Zarzana K J, Rudich Y and Brown S S 2016 *Atmos. Meas. Tech.* **9** 41

[10] Venables D S, Gherman T, Orphal J, Wenger J C and Ruth A A 2006 *Environ. Sci. Technol.* **40** 6758

[11] Werle P, Mücke R and Slemr F 1993 *Appl. Phys. B* **57** 131

[12] Osthoff H D, Brown S S, Ryerson T B, Fortin T J, Lerner B M, Williams E J, Pettersson A, Baynard T, Dubé W P, Ciciora S J and Ravishankara A R 2006 *J. Geophys. Res.* **111** D12305

[13] Wojtas J, Mikolajczyk J and Bielecki Z 2013 *Sensors* **13** 7570

[14] Brown S S, Stark H and Ravishankara A R 2002 *Appl. Phys. B* **75** 173

[15] Brown S S, Stark H, Ciciora S J and Ravishankara A R 2001 *Geophys. Res. Lett.* **28** 3227

[16] Kebabian P L, Wood E C, Herndon S C and Freedman A 2008 *Environ. Sci. Technol.* **42** 6040

[17] Matsumi Y, Murakami S, Kono M, Takahashi K, Koike M and Knodo Y 2001 *Anal. Chem.* **73** 5485

[18] Matsumoto J and Kajii Y 2003 *Atomos. Environ.* **37** 4847

[19] Bradshaw J, Davis D, Crawford J, Chen G, Shetter R, Müller M, Gregory G, Sachse G, Blake D, Heikes B, Singh H, Mastromarino J and Sandholm S 1999 *Geophys. Res. Lett.* **26** 471

[20] Ryerson T B, Williams E J and Fehsenfeld F C 2000 *J. Geophys. Res.* **105** 26447

[21] Sanders S E, Willis O R, Nahler N H and Wrede E 2018 *J. Chem. Phys.* **149** 014201

[22] Mizouri A, Deng L Z, Eardley J S, Nahler N H, Wrede E and Carty D 2013 *Phys. Chem. Chem. Phys.* **15** 19575

[23] Harrison R M 2018 *Npj Clim. Atmos. Sci.* **1** 5

[24] Sugimoto N, Takeuchi N, Iijima H, Arai T and Takezawa S 1984 *Chem. Phys. Lett.* **106** 403

[25] Vandaele A C, Hermans C, Simon P C, Van Roozendael M, Guilmot J M, Carleer M and Colin R 1996 *J. Atmos. Chem.* **25** 289

[26] Evertsen R, Staicu A, Dam N, Van Vliet A and Ter Meulen J J 2002 *Appl. Phys. B: Lasers Opt.* **74** 465

[27] Burrows J P, Dehn A, Deters B, Himmelmann S, Richter A, Voigt S and Orphal J 1998 *J. Quantun. Spectrosc. Radiat. Transfer* **60** 1025